Chapter 10
Bacteriophage RNA Polymerases

Ritwika S. Basu and Katsuhiko S. Murakami

Abstract Bacteriophage-encoded RNA polymerase (RNAP) was first discovered in T7 phage infected *Escherichia coli* cells. It was known that phage infection on host bacterial cells led to redirection of the host gene expression towards generation of progeny phage particles, but a previously uncharacterized "switching event" leading to the expression of late bacteriophage genes was first attributed to a phage-encoded RNAP. This phage RNAP could recognize promoters on the phage genome and express phage genes using a single-polypeptide polymerase of ~100 kDa molecular weight, which is ~4 times smaller than bacterial RNAPs. This was a substantial simplification from the previously known RNAPs from bacteria (5 subunits) and eukaryotes (more than 12 subunits); nonetheless, the single-unit T7 RNAP is able to recognize promoter DNA and unwind double-stranded (ds) DNA to form open complex, and after abortive initiation, it proceeds to processive RNA elongation. The simplicity of T7 phage RNAP made it an ideal model system to study the transcription mechanism and an ideal tool for protein expression system in bacterial cells. In this chapter, we will review the current state of knowledge of transcription mechanism in single-unit bacteriophage RNAPs from the two deeply studied T7 and the N4 phage RNAPs.

Keywords RNA polymerase • Transcription • Bacteriophage • T7 • N4

R.S. Basu • K.S. Murakami (✉)
Department of Biochemistry and Molecular Biology, The Pennsylvania State University, University Park, PA 16802, USA

The Center for RNA Molecular Biology, The Pennsylvania State University, University Park, PA 16802, USA
e-mail: kum14@psu.edu

K.S. Murakami and M.A. Trakselis (eds.), *Nucleic Acid Polymerases*, Nucleic Acids and Molecular Biology 30, DOI 10.1007/978-3-642-39796-7_10,

10.1 T7 RNAP Structure: The Prototype of Single-Unit RNAP

The first crystal structure of RNAP was determined in 1993 from the single-unit bacteriophage T7 RNAP (Sousa et al. 1993). The domain organization of the T7 RNAP was found similar to the bacterial DNA polymerase (DNAP) I (Arnold et al. 1995), e.g., Klenow fragment (KF) of DNA Pol I (Fig. 10.1). The structure resembles the anatomy of a right hand comprising of palm, fingers, and thumb subdomains that are arranged around a DNA-binding cleft. In addition, an N-terminal domain (NTD) constitutes the front wall of the DNA-binding cleft, making the DNA-binding cleft deeper and narrower in RNAP, and also plays roles in promoter recognition and DNA unwinding for making transcription-competent open complex.

The palm subdomain (Fig. 10.1a) forms the base of the DNA-binding cleft with the fingers and the tall thumb subdomains forming either sidewalls of the channel. Invariant residues from motifs A, B, and C cluster around this catalytic cleft. Aspartate residues, conserved in all nucleic acid polymerases, bear the most important catalytic function of chelating two divalent metals (Mg^{2+}) at the active site. The catalytic metal A (Me_A) generates the nucleophile at the 3′-end RNA for the S_N2 nucleotidyl transfer reaction, and a nucleotide-binding metal (Me_B) stabilizes the charge distribution of the incoming nucleotide at the reaction transition state (Steitz et al. 1994; Sect. 10.3.3; Fig. 10.4).

10.1.1 Promoter Binding

The T7 promoter sequence is conserved from the −17 to +6 position with a highly AT-rich region centered around −17. The upstream duplex-form DNA from −17 to −5 binds to the NTD, and the DNA bases downstream are melted and a single-stranded template DNA is directed into the active site. T7 RNAP recognizes the promoter through three main interactions (Fig. 10.2a): (1) DNA bases are recognized by an antiparallel β-hairpin of the fingers, the specificity loop, from the major groove; (2) an AT-rich recognition motif in the NTD recognizes AT-rich (−17) region by inserting a flexible surface loop into the DNA minor groove; (3) the intercalating β-hairpin in the NTD melts the promoter DNA and marks the upstream edge of the transcription bubble. This precise location of the transcription bubble ensures correct positioning of the transcription start site DNA base at the active site. At this point, RNAP is ready to accept the two nucleotides that form base pairs with the +1 and +2 template DNA bases to initiate RNA synthesis.

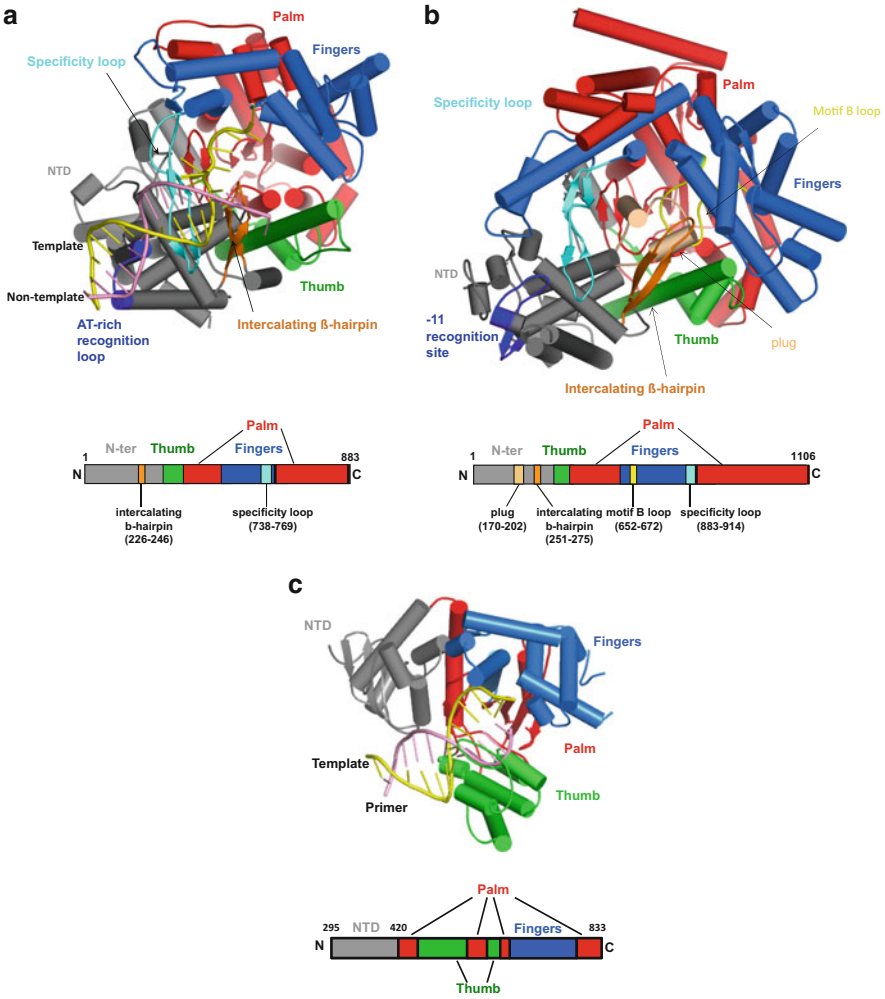

Fig. 10.1 Structures of single-unit DNA-dependent polymerases. Right hand-like organization domains in T7 RNAP complexed with promoter DNA (**a**), N4 mini-vRNAP (**b**), and KlenTaq DNAP I (**c**) are shown. Same orientation of the structures were obtained by superposing the palm domains. The palm (*red*), fingers (*blue*), thumb (*green*) domains, and NTD (*gray*) are shown as *cylinders* (α-helix) and *arrows* (β-strands). Double-stranded promoter DNA containing template (*yellow*) and non-template (*pink*) in T7 RNAP and the primer (*pink*) template (*yellow*) duplex in KlenTaq reach the active site cleft formed by three β-strands. Active site of N4 mini-vRNAP (**b**) is blocked by the plug (*wheat*) and the motif B loop (*yellow*). The primary structures of the polymerases are shown below each 3-D structure with the same color code

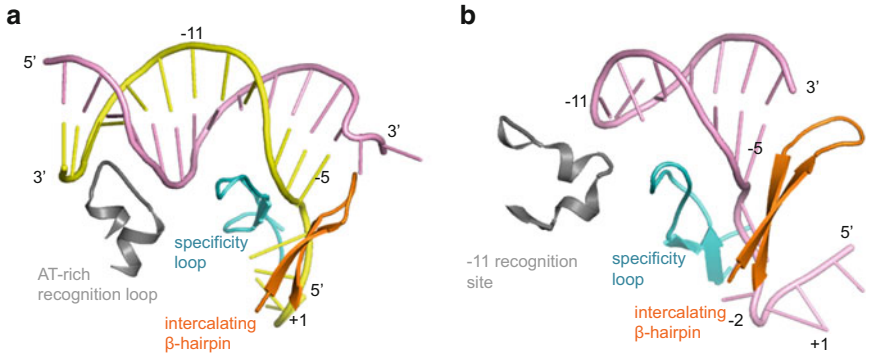

Fig. 10.2 Structural motifs for promoter recognition. (**a**) AT-rich recognition loop (*gray*), specificity loop (*cyan*), and intercalating hairpin (*orange*) in T7 RNAP binary complex. Template (*yellow*) and non-template (*pink*) are shown. (**b**) −11 recognition loop (*gray*), specificity loop (*cyan*), and intercalating hairpin (*orange*) in the N4 RNAP binary complex recognize the hairpin promoter (*pink*). The figure has been adapted from Gleghorn et al. (2008)

10.1.2 Transcript Initiation

The structure of T7 RNAP transcription initiation complex (Cheetham and Steitz 1999) showed how RNAP positions the template DNA bases at the active site at every subsequent step of NTP addition. In this structure, RNAP was bound to a 17-bp duplex promoter and a 3-mer RNA transcript base-paired with the single-stranded tailed template.

The presence of RNA in this polymerase structure offered an insight into the rNTP-specific RNA synthesis. In contrast to DNAP, a bulky glutamate "steric gate" near the active site is replaced to a glycine in RNAP that makes space for the 2′-OH of incoming NTP. Secondly, a carbonyl group of the active site amino acid residues hydrogen bonds with the 2′-OH of the 3′ primer end allowing only 3′-endo ribose conformation of the base. Further, the DNA-binding pocket is also complementary to the A-form DNA/RNA heteroduplex thus favoring the formation of DNA/RNA heteroduplex at the stage of RNA extension.

The promoter contacts are maintained, while the DNA/RNA heteroduplex accumulates in the active site, positioning the growing primer end at the active site. Accordingly, the −1 template base that stacked with the +1 template for proper positioning during *de novo* initiation assumes a flipped out conformation allowing transcript extension to RNA 3-mer stage. This observation served the first structural evidence for the "DNA scrunching" mechanism during initiation. The primer DNA scrunches into the active site through the initial synthesis phase until it chooses one of the two fates, abortive or productive transcription. During initiation, abortive transcripts are displaced from the template by collapsing the newly formed bubble due to small, weak DNA/RNA hybrids (Brieba and Sousa 2001). Alternatively, it could extend the DNA/RNA hybrid and scrunch it until it reaches the threshold

length of 8 nt, after which the entire complex undergoes a phenomenal conformational change into a processive elongation complex (Sect. 10.2).

10.2 Transcription Elongation

Two structures of T7 RNAP with 8-mer (Tahirov et al. 2002) and 11-mer (Yin and Steitz 2002) RNAs provide a holistic view of how the features of a transcription elongation complex emerge from the initiation complex after extensive reorganizations of the RNAP and DNA structures. A transcribing complex is committed to elongation when it has successfully accommodated numerous concurrent events including promoter release, partial collapse of the bubble, construction of an RNA exit channel, and peeling of the 5′ end of the nascent RNA from the template DNA. The threshold length of DNA/RNA hybrid determining this transition to elongation had been only predicted from biochemical observations, but in both the transcription elongation structures, the nascent RNA forms a heteroduplex with the template DNA of only 8 bp, upstream of which is peeled off the template and directed into a new formed exit channel.

10.2.1 Promoter Release and Processivity

The NTD being most closely involved in interaction with the promoter undergoes major rearrangement. On comparing the RNAP in the initiation and elongation stages, three subdomains in the NTD show independent rearrangement movements (Fig. 10.3). (1) A six-helix bundle called the promoter-binding domain (PBD) undergoes a massive rigid body rotation of 140° to a position previously occupied by the promoter, thereby destroying its promoter interaction sites. Along with PBD, the adjacent intercalating β-hairpin, an important motif for promoter melting in initiation, also becomes disordered in this promoter release event. (2) An α-helix (named C-helix) at the N-terminus of NTD nearly doubles in length by stacking of two smaller helices seen during initiation, forming part of the binding site for DNA/RNA hybrid. This helix protrudes into the region occupied by the PBD in initiation suggesting the concerted nature of the two motions. (3) Subdomain H undergoes extensive refolding into two antiparallel helices, paired with a large translation of 70 Å to the opposite side of the polymerase, forming the rim of the RNA exit channel on one side, and interacts with the non-template DNA from its opposite surface.

The formation of the RNA exit channel is the most important determinant of transcription processivity. Along with the subdomain H, two important motifs are involved in its formation including the thumb and the specificity loop. The interaction of the channel wall with RNA is only through salt bridges between the phosphate backbone and basic residues of specificity loop and subdomain H.

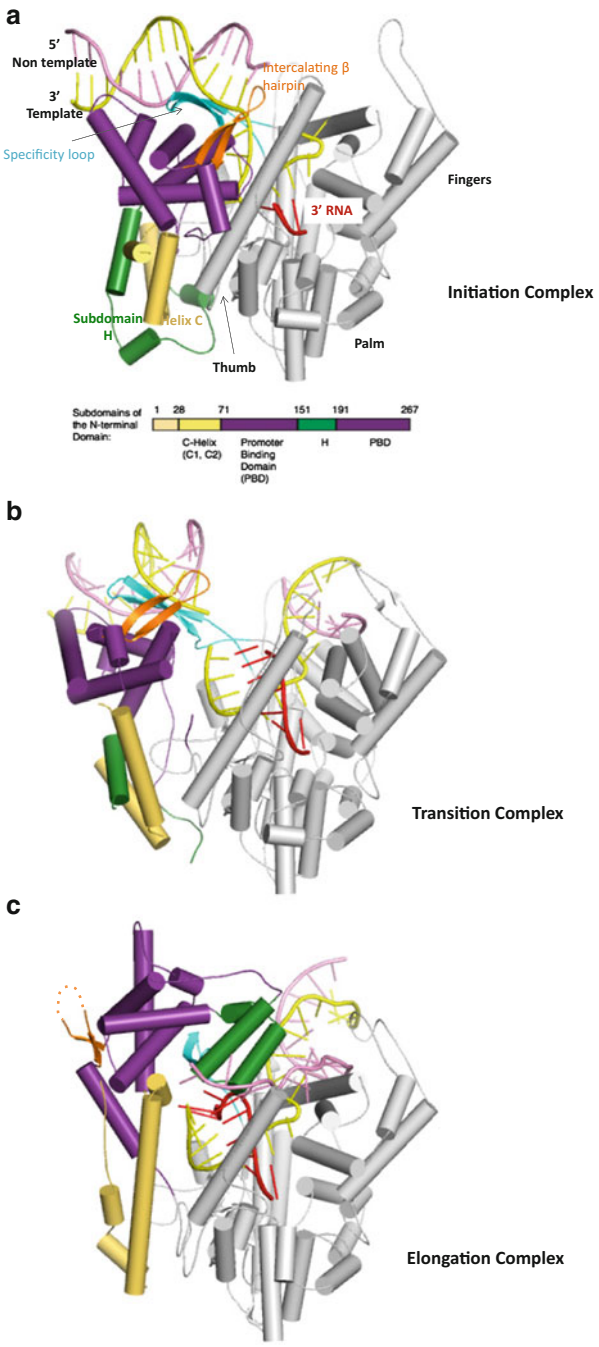

Fig. 10.3 Comparison of the structures of initiation complex (**a**), intermediate complex (**b**), and elongation complex (**c**). α-helices are represented by *cylinders* and β-sheets by *arrows*, while disordered regions are shown in *dotted lines*. The structures are similarly oriented by superposing the palm domains including the active site. Transition involves major conformational changes in the NTD colored as independently moving regions: promoter-binding domain (*purple*), intercalating hairpin (*orange*), helix C motif (*pale yellow*), and subdomain H (*green*). The CTD (*gray*) remains mostly unchanged except for movements in the long thumb helix and the specificity loop (*cyan*). The template strand is *yellow*, non-template is *pink*, and RNA is *red*. The downstream DNA is highly bent with respect to the upstream regions to help bubble formation (**c**). The primary structure of the NTD subdomains is also shown with the same color code (**a**). These figures have been adapted from Yin and Steitz (2002)

Processivity is also favored over abortive transcription due to the extensive interactions of the 7 bp DNA/RNA heteroduplex with its binding site.

Transcription processivity is coupled with the continuous downstream progress of the transcription bubble. At the onset of transcription, the bubble is generated from the unwinding of the downstream duplex DNA, approximately through 146° with respect to the upstream promoter. The template strand also plunges deep into the active site and comes out by bending about 80° at the upstream and downstream end of the bubble (Fig. 10.3c).

10.2.2 Transition to Elongation Complex

Transition from the initiation to elongation complexes should involve metastable complexes that not only form the basis of abortive cycling but also assume the conformation of an expanded active site to accumulate a growing DNA/RNA hybrid of about 8 nt length (Huang and Sousa 2000; Temiakov et al. 2000) while still bound to the promoter. Biochemical studies proposed that the transition was two steps (Bandwar et al. 2007; Guo et al. 2005; Ma et al. 2005), where RNA extended to about 8 nt followed by major refolding events accompanying synthesis of 9–14 nt (Tang et al. 2008). One of the intermediate structures with a 17-mer promoter DNA and 7-mer RNA transcript in a bubble showed the nature of transition between the vastly different initiation and elongation complexes (Durniak et al. 2008; Fig. 10.3b). This structure was captured using a mutant (P266L) in a loop connecting the polymerase NTD and C-terminal domains.

In the first stage of transition, NTD movements including PBD and helix C appear to have proceeded halfway, leading to the enlargement of the active site to accommodate the 7-bp DNA/RNA hybrid. Subdomain H of NTD, however, remains in its initiation orientation. The second stage of transition involves a final movement of the NTD, specificity loop, and subdomain H that loses promoter contact, completes the exit channel formation, and also forces the downstream duplex to its bent position.

10.2.3 Nucleotide Addition Cycle

In every nucleotide addition cycle, RNAP sieves through the pool of NTPs for the correct substrate through its intricate mechanism of nucleotide selection. The catalytic-competent nucleotide-binding N-site elicits the nucleotidyl transfer reaction between the RNA primer 3′-end base at P-site and the incoming NTP to extend the RNA through one base. The extended RNA then translocates upstream relative to the active site, opening the N-site for the next round of cycle. T7 RNAP conducts this harmonized process through fine regulation by elements mainly from the fingers and palm subdomain. Crystal structures of T7 RNAP complexes with the

DNA, RNA, and nucleotide provide great insights into its nucleotide addition cycle (Yin and Steitz 2004; Temiakov et al. 2004).

10.2.3.1 Substrate Selection in Pre-insertion Site

Structure of a ternary elongation complex with non-hydrolyzable ATP analog identified a "pre-insertion site" for a substrate binding prior to catalytically competent nucleotide binding at the "insertion" N-site (Temiakov et al. 2004; Fig. 10.4a). The pre-insertion site is linked to the "open" conformation of a conserved O-helix of the fingers. In this conformation, the templating base faces away from its accepting position, and the conserved tyrosine residue at the end of the O-helix meanwhile blocks the nucleotide insertion site. The tyrosine hydroxyl group interacts with the 2′-OH of the substrate, forming the primary discrimination of incoming rNTPs against dNTPs. The substrate is bound along the O-helix but is not Watson–Crick paired with the template DNA base, implying that the pre-insertion site is an early fidelity checkpoint.

10.2.3.2 Substrate Loading at the Catalytic Site

Substrate loading from the pre-insertion site to the catalytic insertion site is achieved by "closing of the fingers," wherein rotation of the O-helix is the most significant. Structure of a pre-catalytic substrate complex trapped with the use of a nonreactive nucleotide analog showed the nature of O-helix movement when substrate was loaded onto the catalytic insertion site (N-site) and thereby defined the closed conformation of the fingers (Yin and Steitz 2004). The O-helix rotates about a pivot point at its middle, causing the amino end of the helix to close onto the substrate triphosphate moiety, stabilized in this position through positive charge from lysine and arginine residues. Simultaneously, the opposite end of the O-helix, including the important tyrosine residue, moves away to make space for the base moiety of the incoming substrate. The base specific and ribose discriminating interactions of the pre-insertion site are maintained in the closed conformation to face a final round of fidelity check.

The incoming substrate alignment for catalysis, in the active site, is maintained not only by the O-helix residues but also by the accompanying nucleotide-binding metal Me_B, which is, in turn, positioned by chelating the conserved active site aspartates. Further, the octahedral coordination of catalytic metal ion Me_A maintains the critical alignment of the reactive groups, 3′ OH of primer terminus and 5′ αP of incoming substrate. The mechanism of nucleotidyl transfer reaction, which extends one RNA base and produces a pyrophosphate (PPi) by-product, will be described in Sect. 10.3.3.

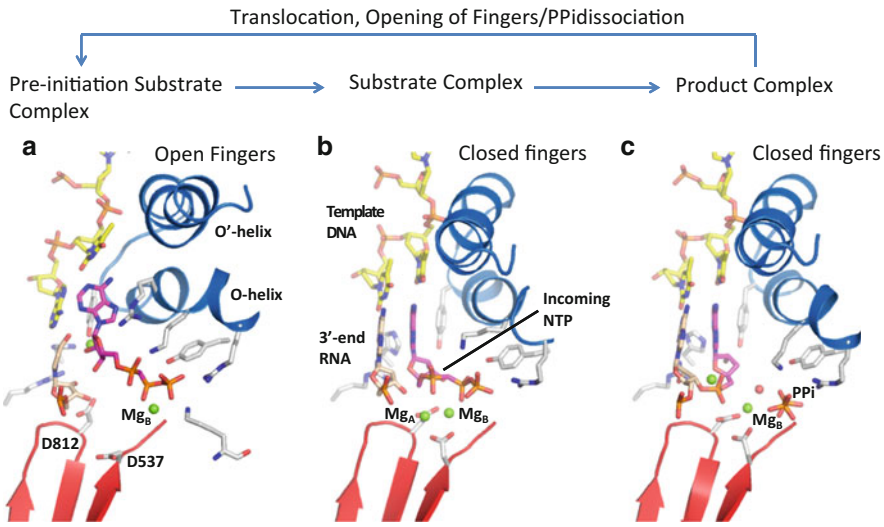

Fig. 10.4 Active site views during nucleotide addition cycle. Structures of the preinitiation complex (PDB: 1S07) (**a**), substrate complex (PDB: 1S76) (**b**), and product complex (PDB: 1S77) (**c**) are aligned similarly by superposing the palm. Important motifs (*ribbons*) and amino acid residues (*sticks*) are shown. Helix O and O′ from fingers (*blue*) and motifs A and C (*red*) from the palm provide amino acid side chains to bind the incoming nucleotide (*magenta* carbons), magnesium atoms (*green spheres*), or transcript primer end (*light pink* carbons). The template DNA is shown as *sticks* with *yellow* carbon atoms

10.2.3.3 Translocation

After the addition of a base to the transcript, the final step of the nucleotide addition cycle is the translocation of the DNA/RNA hybrid through one base distance such that the 3′-end RNA positions in the P-site. The structure of a post-catalytic, pre-translocated product complex, isolated right after phosphodiester bond formation but before dissociation of nascent PPi, showed that the phosphodiester bond does not cause any change in the RNAP or DNA/RNA hybrid (Fig. 10.4c). In the post-translocated state, the only difference lies in the dissociation of PPi along with the coordinated Me_B, which breaks the interactions with the O-helix residues and thus favors the open state. Moreover, the rNTP discriminator tyrosine at the O-helix moves towards the heteroduplex and stacks with the primer end base preventing backtracking of the hybrid, while opening the triphosphate site due to the pivoted helix motion. It is thus proposed that translocation of DNA/RNA hybrid in single-unit RNAP is coupled with PPi dissociation which leads to the opening of O-helix for the next round of nucleotide addition, often called the power-stroke mechanism of translocation (Jiang and Sheetz 1994).

10.3 N4 vRNAP: Factor-Dependent Single-Unit Polymerase

While the characterization of T7-related RNAP was progressing rapidly, the discovery of a unique phage-encoded, virion-encapsidated RNAP (vRNAP) isolated from a lytic coliphage N4 (Falco et al. 1977) added breadth to the studies of single-unit RNAPs. In contrast to other phage RNAPs, N4 vRNAP is encapsulated within the virion to being injected into the bacterial cell at the onset of infection. Upon injection of the N4 double-stranded DNA genome, host proteins DNA gyrase and single-stranded DNA-binding protein (EcoSSB) prepare the N4 vRNAP specific promoter comprising a DNA hairpin with a 5–7-base pair stem and 3-base loop (Glucksmann-Kuis et al. 1996; Haynes and Rothman-Denes 1985). This DNA hairpin promoter is a key to activate the co-injected vRNAP from transcription-inactive state. After transcription initiation, N4 vRNAP depends on EcoSSB for transcript elongation, which displaces nascent RNA transcripts from the template DNA for recycling (Davydova and Rothman-Denes 2003). Thus the part of NTD responsible for RNA separation in T7 transcription elongation (see Sect. 10.3.1) was absent in N4 vRNAP. EcoSSB could thus be termed as a transcription factor, and N4 vRNAP has been emerged as an important model for studying the structural basis of transcription activation as well as factor-dependent transcription of the single-unit RNAP.

Much larger than other phage RNAPs, the 320 kDa N4 vRNAP can be divided into three domains, and a central polymerase domain of 1100 amino acid (called mini-vRNAP) exhibits transcription initiation, elongation, and termination properties identical to full-length vRNAP (Kazmierczak et al. 2002). Sequence alignment classified the N4 mini-vRNAP as the most divergent member of the single-unit RNAP family. There is only small sequence similarity with other members except the catalytically important motifs A, B, C, and T/DxxGR.

10.3.1 Structure of N4 vRNAP

Studies of the structure and function of N4 mini-vRNAP advanced the scope of single-unit RNAP studies. Despite a lower sequence similarity, the N4 mini-vRNAP structure was highly similar to the T7 RNAP structure (Murakami et al. 2008) (Fig. 10.1b). It reiterated the modular organization of the right hand-like structure, with the same subdomains surrounding the DNA-binding cleft and the same structural motifs. However, the promoter recognition motifs in the fingers and NTD, although similar, had adapted interactions specific for the special hairpin N4 promoter (Sect. 10.3.2).

The two major differences between the N4 vRNAP and T7 RNAP structures are the presence of a plug module insertion in the NTD and a loop inserted in the middle of motif B (motif B loop) found in the N4 vRNAP. The plug and motif B

loop interact with the motifs A and C of palm that cover all catalytically essential amino acid residues of N4 vRNAP active site until the hairpin-form promoter DNA interacts and activates the polymerase.

10.3.2 Unique Hairpin Promoter DNA Recognition

The N4 vRNAP recognizes hairpin-form promoter DNA by using (1) −11 base recognition motif in the NTD, which recognizes the tip of hairpin loop, (2) specificity loop from the fingers that contact the hairpin from the major groove, and (3) intercalating β-hairpin to maintain the junction of the double- and single-stranded DNA (Fig. 10.2b). After binding the hairpin-form promoter DNA, the N4 vRNAP changes its conformation including a rigid body movement of the plug away from the active site and the motif B loop refolding outwards from the active site, which turns the residues on the O-helix for incoming NTP binding. The hairpin promoter-bound N4 vRNAP conformation is competent for transcription.

10.3.3 Nucleotidyl Transfer Reaction

The nucleotidyl transfer reaction by DNA and RNA polymerases follows a generalized mechanism of two-metal catalysis (Steitz et al. 1994), wherein the catalytic metal (Me_A) is known to work as a Lewis acid to enhance the nucleophilicity of the 3′ oxygen attacking group of the primer 3′ end, initiating the S_N2 reaction onto the 5′ αP of the incoming nucleotide. The nucleotide-binding metal (Me_B) is coordinated by the triphosphates of the incoming NTP, stabilizing the pentacovalent transition state.

In case of the transcription initiation, two NTP substrates bind to the empty P- and N-sites concurrently to form the first phosphodiester bond formation at the 5′-end RNA. The structural snapshots (Gleghorn et al. 2011), Raman crystallography (Chen et al. 2011), and time-resolved trigger-freeze crystallography (Basu and Murakami 2013) studies of ternary complexes of N4 mini-vRNAP during transcript initiation provide the most updated and complete knowledge of the reaction mechanism (Fig. 10.5). Two forms of pre-catalytic substrate complexes could be isolated; while both contained the two initiating nucleotides at the P- and N-sites, the catalytic metal (Me_A) was absent in one of them. This intermediate showed the important, final molecular rearrangements in the active site elicited by the critical Me_A binding to allow catalysis. In the absence of Me_A, the 3′ O from GTP (+1) and the 5′ αP of GTP (+2) were beyond reacting distance (4.1 Å) and were bought closer only with the binding of Me_A (Fig. 10.5b, c). This observation proposed that the catalytic metal binding, which is sensitive to its octahedral coordination requirements, serves as a final fidelity checkpoint where a fine misalignment of

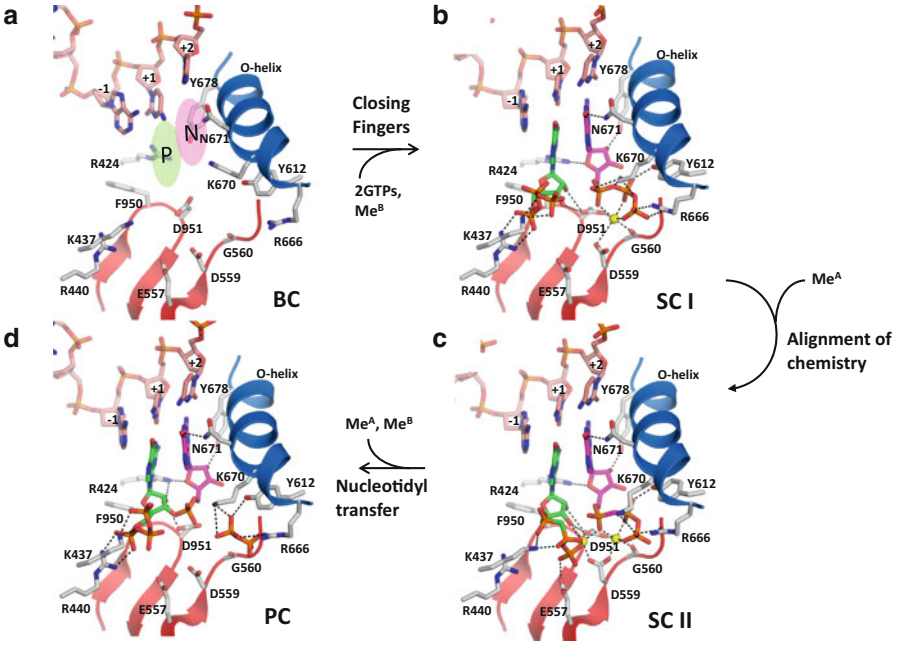

Fig. 10.5 Structures of active site, DNA and nucleotides during nucleotidyl transfer reaction. The main chains (*ribbon models*) of motifs A and C (*red*) and of the O-helix (*blue*) and the main and side chains (*stick models*) involved in nucleotide and metal binding in the promoter binary complex (**a**), substrate complex I (**b**), substrate complex II (**c**), and product complex (**d**). NTP binding P- and N-sites are indicated as *green* and *magenta circles* in **a**. DNA template (from −1 to +2, *pink*) and nucleotides at +1 (*green*) and +2 (*magenta*) positions are shown as *stick models*. Divalent metals are depicted by *yellow spheres*. Hydrogen bonds and salt bridges are depicted by *black dashed lines* (Gleghorn et al. 2011)

the 5′ αP of a mispaired incoming nucleotide disallows the Me_A binding and thereby prevents the catalysis.

Consistent with the steps in transcript elongation, the O-helix in the initiation complexes was in a closed state, providing its basic residues for stable interactions with the nucleotide at N-site. Additionally, the stability of the nucleotide binding at the P-site, an initiation-specific event, could be explained by electrostatic interactions of basic residues of the palm with the triphosphates and the partial base stacking with a purine at −1 template DNA position. Furthermore, the γP group of GTP (+1) participates in the Me_A octahedral coordination. Loss of affinity and catalytic activity with GDP (+1) compared with GTP (+1), led to the proposition of substrate-assisted catalysis for the first phosphodiester bond formation mediated by the γP group and Me_A binding.

A time course soak-trigger-freeze crystallographic study on this transcript initiation process provided the most direct real-time trace of the unperturbed events in the nucleotidyl transfer reaction (Basu and Murakami 2013). The observation of polymerase reaction in real time by high-resolution X-ray crystallography showed

that the nucleotide binding, the O-helix closure, and template DNA rearrangement were completed at early stages of reaction. Subsequently, the catalytic metal binding rearranges the reactive groups just prior to the phosphodiester bond formation. Owing to the sensitivity of Me_A for its octahedral coordination, its binding is subject to correct Watson–Crick pairing of the incoming nucleotide, and for the same reason it leaves the active site right after a phosphodiester bond formation, thereby also preventing the backward cleavage reaction.

References

Arnold E, Ding J, Hughes SH, Hostomsky Z (1995) Structures of DNA and RNA polymerases and their interactions with nucleic acid substrates. Curr Opin Struct Biol 5:27–38

Bandwar RP, Ma N, Emanuel SA, Anikin M, Vassylyev DG, Patel SS, McAllister WT (2007) The transition to an elongation complex by T7 RNA polymerase is a multistep process. J Biol Chem 282:22879–22886

Basu RS, Murakami KS (2013) Watching the bacteriophage N4 RNA polymerase transcription by time-dependent soak-trigger-freeze X-ray crystallography. J Biol Chem 288:3305–3311

Brieba LG, Sousa R (2001) T7 promoter release mediated by DNA scrunching. EMBO J 20:6826–6835

Cheetham GM, Steitz TA (1999) Structure of a transcribing T7 RNA polymerase initiation complex. Science 286:2305–2309

Chen Y, Basu R, Gleghorn ML, Murakami KS, Carey PR (2011) Time-resolved events on the reaction pathway of transcript initiation by a single-subunit RNA polymerase: Raman crystallographic evidence. J Am Chem Soc 133:12544–12555

Davydova EK, Rothman-Denes LB (2003) Escherichia coli single-stranded DNA-binding protein mediates template recycling during transcription by bacteriophage N4 virion RNA polymerase. Proc Natl Acad Sci USA 100:9250–9255

Durniak KJ, Bailey S, Steitz TA (2008) The structure of a transcribing T7 RNA polymerase in transition from initiation to elongation. Science 322:553–557

Falco SC, Laan KV, Rothman-Denes LB (1977) Virion-associated RNA polymerase required for bacteriophage N4 development. Proc Natl Acad Sci USA 74:520–523

Gleghorn ML, Davydova EK, Rothman-Denes LB, Murakami KS (2008) Structural basis for DNA-hairpin promoter recognition by the bacteriophage N4 virion RNA polymerase. Mol Cell 32:707–717

Gleghorn ML, Davydova EK, Basu R, Rothman-Denes LB, Murakami KS (2011) X-ray crystal structures elucidate the nucleotidyl transfer reaction of transcript initiation using two nucleotides. Proc Natl Acad Sci USA 108:3566–3571

Glucksmann-Kuis MA, Dai X, Markiewicz P, Rothman-Denes LB (1996) E. coli SSB activates N4 virion RNA polymerase promoters by stabilizing a DNA hairpin required for promoter recognition. Cell 84:147–154

Guo Q, Nayak D, Brieba LG, Sousa R (2005) Major conformational changes during T7RNAP transcription initiation coincide with, and are required for, promoter release. J Mol Biol 353:256–270

Haynes LL, Rothman-Denes LB (1985) N4 virion RNA polymerase sites of transcription initiation. Cell 41:597–605

Huang J, Sousa R (2000) T7 RNA polymerase elongation complex structure and movement. J Mol Biol 303:347–358

Jiang MY, Sheetz MP (1994) Mechanics of myosin motor: force and step size. Bioessays 16:531–532

Kazmierczak KM, Davydova EK, Mustaev AA, Rothman-Denes LB (2002) The phage N4 virion RNA polymerase catalytic domain is related to single-subunit RNA polymerases. EMBO J 21:5815–5823

Ma K, Temiakov D, Anikin M, McAllister WT (2005) Probing conformational changes in T7 RNA polymerase during initiation and termination by using engineered disulfide linkages. Proc Natl Acad Sci USA 102:17612–17617

Murakami KS, Davydova EK, Rothman-Denes LB (2008) X-ray crystal structure of the polymerase domain of the bacteriophage N4 virion RNA polymerase. Proc Natl Acad Sci USA 105:5046–5051

Sousa R, Chung YJ, Rose JP, Wang BC (1993) Crystal structure of bacteriophage T7 RNA polymerase at 3.3 A resolution. Nature 364:593–599

Steitz TA, Smerdon SJ, Jager J, Joyce CM (1994) A unified polymerase mechanism for nonhomologous DNA and RNA polymerases. Science 266:2022–2025

Tahirov TH, Temiakov D, Anikin M, Patlan V, McAllister WT, Vassylyev DG, Yokoyama S (2002) Structure of a T7 RNA polymerase elongation complex at 2.9 A resolution. Nature 420:43–50

Tang GQ, Roy R, Ha T, Patel SS (2008) Transcription initiation in a single-subunit RNA polymerase proceeds through DNA scrunching and rotation of the N-terminal subdomains. Mol Cell 30:567–577

Temiakov D, Mentesana PE, Ma K, Mustaev A, Borukhov S, McAllister WT (2000) The specificity loop of T7 RNA polymerase interacts first with the promoter and then with the elongating transcript, suggesting a mechanism for promoter clearance. Proc Natl Acad Sci USA 97:14109–14114

Temiakov D, Patlan V, Anikin M, McAllister WT, Yokoyama S, Vassylyev DG (2004) Structural basis for substrate selection by t7 RNA polymerase. Cell 116:381–391

Yin YW, Steitz TA (2002) Structural basis for the transition from initiation to elongation transcription in T7 RNA polymerase. Science 298:1387–1395

Yin YW, Steitz TA (2004) The structural mechanism of translocation and helicase activity in T7 RNA polymerase. Cell 116:393–404